Identification of Drag Force of the Underwater Vehicles

Y. Jahangardy[†], R. Madoliat and N. M. Nouri

Iran University of Science and Technology, Tehran, Iran

†*Corresponding Author Email: Jahangardy@iust.ac.ir*

ABSTRACT

An inverse analysis is conducted for the estimation of drag coefficient and wake's width in incompressible turbulent flows over the moving underwater bodies. The inverse analysis uses the laws of momentum and mass conservation for a control volume to estimate the drag coefficient and the wake's width from the measured velocity in the wake. The drag coefficient and wake's width are determined as unknown parameters by the Levenberg–Marquardt algorithm. The proposed inverse method is applicable for an environment without boundaries (e.g., the sea). Several experiments are conducted to evaluate the developed inverse algorithm. The wake velocity behind a cylinder located in the flow field is measured by a calibrated pitot tube and is used as an input to the algorithm. The cylinder is selected as the test body, because its hydrodynamic information is available in the literature. The effects of the tunnel's wall and the turbulence intensity are considered in the results of the algorithm. The estimated drag coefficient is validated by the values presented in the literature. The estimated wake-velocity profiles are fitted favorably with the measured velocities at the corresponding locations. It is shown that the proposed inverse method can be used to estimate the drag coefficient and wake's width of the underwater vehicles with very good accuracy.

Keywords: Inverse method; Drag force identification; Wake velocity profile.

1. INTRODUCTION

Several new researches have been dedicated to study the hydrodynamic forces specially drag force, acting on the moving underwater bodies and some of them are devoted to develop the drag reduction methods (Jordan, 2014; Amromin, 2013; Yang and Ding, 2014; Akindoyo and Abdulbari, 2016; Ghassabi and Kahrom, 2015; Jafargholinejad *et al.* 2011). Great attentions of scientists to identify hydrodynamic forces show the importance of development of force prediction methods. Due to the difficulties and high cost of direct measurement of hydrodynamic forces, they can be estimated by some indirect methods, such as the inverse algorithms. This study focuses on drag prediction by an Inverse method.

Inverse problems have originated in the heat transfer community in connection with the estimation of surface heat flux histories from measured temperature histories inside a heat conducting body. Inverse heat-conduction problems have been studied mostly for the estimation of unknown boundaries or initial conditions, thermo-physical properties, the strength of heat sources, and geometrical configurations (Alifanov, 1994; Ozisik, and Orlande, 2000). To date, a variety of numerical

and analytical techniques, such as Tikhonov regularization method, the function specification method and the mollification, has been developed for solving inverse heat conduction problems. Despite many potential applications, it only has been in recent years that inverse heat convection problems have received some attention.

Inverse problems of laminar forced convection in ducts have been studied for estimation of initial temperature profile, wall heat flux and thermo-physical properties (Grysa *et al.* 2014; Helcio, 2012). Su *et al.* (2000) used the Levenberg-Marquardt method to estimate non-uniform wall heat fluxes in steady-state, thermally-developing, hydro-dynamically-developed turbulent flow in a circular pipe by using the temperature measurements obtained at several different locations in the stream. Later, Su and Silva (2001) solved an inverse heat convection problem to estimate simultaneously the inlet temperature profile and the wall's heat flux distribution in a steady-state, thermally-developing, hydro-dynamically-developed turbulent flow in a circular pipe by using the Levenberg-Marquardt method and the temperature measurements taken at different locations in the stream. Sakly *et al.* (2011) developed an Inverse method for Estimation of the

Effective Thermal Properties in a Metallic Medium. They used an iterative procedure, based on minimizing a sum of squares norm with the Levenberg-Marquardt method, to solve the inverse problem.

Recently Inverse problem have been used as a useful method to study different fields such as optimization design of turbo-machines (Yang and Xiao 2013), studying the internal flows (Ahmadabadi *et al.* 2010), measurements (Xiongjun *et al.* 2014) and vibrational systems (Cho and Udwadia 2012). This shows that inverse method has widespread range of application and can be used for solving many problems. However to date no one has developed an Inverse method for drag prediction by means of wake information.

The purpose of the present work is to solve an inverse problem involving the estimation of drag coefficient and wake's width (as unknown parameters) for an incompressible turbulent flow over the underwater bodies by measuring the water velocity in the region of the downstream wake.

Wake of underwater bodies include much information about the flow and body conditions. Several investigations have been done recently for studying the wake of different bodies (Wosnik and Arndt 2013; Morton and Yarusevych 2014). Wake region is produced due to the existence of hydrodynamic forces. Therefore, it must be possible to estimate the hydrodynamic forces from the measured velocity of the wake. To achieve this target, an inverse method is developed that can be used to make reliable predictions of the external forces acting on the body. The least squares method also is used to approximate the unknown parameters. Because of the non-linear objective function, the inverse problem is formulated as a parameter-estimation problem. Its solution is based on minimization of the ordinary least squares, which is done by means of the Levenberg–Marquardt (LM) algorithm.

2. MATHEMATICAL FORMULATION OF THE DIRECT PROBLEM

A body, which is placed in a water flow, reduces the fluid momentum and change the fluid velocity profile. These changes will produce a region called wake region. The velocity profile in this region can be presented by the following equation

$$U_\infty - U_w(y) = K \exp(-y^n) \tag{1}$$

Where U_∞ is the velocity of free flow, $U_w(y)$ is the flow velocity in the wake region, y is the vertical position and K and n are constants. To globalize the results, it is better to make the parameters non-dimensional. When the body is placed symmetrically in the flow, the only force acting on it is drag force. Thus, the velocity profile is symmetric related to y and the power of it (n), in Eq. (1) must be even. Therefore, Eq. (1) can be written as below:

$$\frac{U_\infty - U_w(y)}{U_\infty} = B \exp\left(-\left(\frac{y}{\delta}\right)^2\right) \tag{2}$$

Where δ is the wake's width of the velocity profile and $B=K/U_\infty$. The main reason of reduction velocity in the wake region is the reaction of the drag force acting on the body. Thus, in order to determine the constant B, the momentum and mass conservation laws must be satisfied for a control volume (CV) around the body.
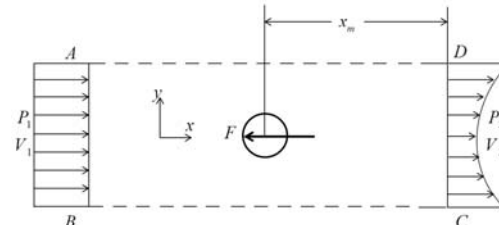

Fig. 1. Control volume around a cylinder.

Present research is done for the estimation of the drag force acting on the underwater vehicles. However, to validate the results of the developed inverse method, the cylinder as an underwater moving body is selected for consideration. This body and its control volume are shown in (Fig. 1). With the incompressible fluid assumption, the mass conservation law can be written as below

$$\int_{c.s} \rho \vec{v}.\vec{n} dA = 0 \tag{3}$$

$$\dot{m}_{side} = \int_{-\infty}^{\infty} \rho U_\infty dA - \int_{-\infty}^{\infty} \rho U_w(y) dA \tag{4}$$

Where ρ and v are the fluid density and velocity respectively, n is the normal vector of surface and $\dot{m}_{side}$ is the mass flux of the CV side. The momentum conservation law is as follow

$$\text{EMBED Equation.DSMT4} \quad \sum F = \int_{c.s} \vec{v} \rho \vec{v}.n dA$$

Where ΣF is the resultant force acting on the cylinder. Because of cylinder symmetry, the only force acting on it is the drag force. Therefore, Eq. (5) can be written as

$$F_d + \int p_\infty dA - \int p_w dA = \dot{M}_{x,out} - \dot{M}_{x,in} \tag{6}$$

Where

$$\dot{M}_{xout} = \rho \int \left[U_\infty^2 - U_\infty U_w(y) + U_w^2(y) \right] dA \tag{7}$$

$$\dot{M}_{x,in} = -\int \rho U_\infty^2 dA \tag{8}$$

p_∞ and p_w are static pressures of the inlet and outlet flow of CV respectively and F_d is the drag force. $\dot{M}_{x,out}$ and $\dot{M}_{x,in}$ are the output and input momentum rates. Therefore, the final format of the momentum conservation law is:

$$-F_d + \int p_\infty dA - \int p_w dA$$
$$= \rho \int (U_w^2(y) - U_\infty U_w(y)) dA \qquad (9)$$

If the pressures of input and output of the CV are equal then the Eq. (9) can be written as below

$$F_d = \rho U_\infty^2 \int \frac{U_w(y)}{U_\infty}(1 - \frac{U_w(y)}{U_\infty}) dA \qquad (10)$$

The assumption of the equality of the entrance and exit pressures for an environment without boundary is acceptable, but in the water tunnel, it is not true and the reliable equation for the tunnel, is Eq. (9). On the other hand, the drag force can be written as

$$F_d = \frac{1}{2} C_d \rho U_\infty^2 A_F \qquad (11)$$

Where C_d is the drag coefficient and A_F is the Frontal area of the body. By substituting Eq. (10) in Eq. (11), the drag coefficient can be achieved as

$$\frac{1}{2} C_d A_F = \int \frac{U_w(y)}{U_\infty}(1 - \frac{U_w(y)}{U_\infty}) dA \qquad (12)$$

If $u = U_\infty - U_w$ then the Eq. (12) can be rewritten as blow

$$\frac{1}{2} C_d A_F = \int \frac{u(y)}{U_\infty}(1 - \frac{u(y)}{U_\infty}) dA \qquad (13)$$

Because $u(y) \ll U_\infty$ the Eq. (13) can be reduced to

$$\frac{1}{2} C_d A_F = \int \frac{u(y)}{U_\infty} dA \qquad (14)$$

In the Cartesian coordinate for the cylinder, A_F and dA can be defined as

$$A_F = DL \qquad (15)$$

$$dA = L dy \qquad (16)$$

Which L and D are the length and diameter of cylinder respectively. Thus, the Eq. (14) can be written as

$$\frac{1}{2} C_d D = \int \left(1 - \frac{U_w}{U_\infty}\right) dy \qquad (17)$$

By solving Eq. (17), the drag coefficient can be derived as below

$$C_d = \frac{2}{D} \int_{-\infty}^{\infty} B \exp(-(\frac{y}{\delta})^2) dy \qquad (18)$$

$$C_d = \frac{2\sqrt{\pi} B \delta}{D} \Rightarrow B = \frac{C_d D}{2\sqrt{\pi}\delta} \qquad (19)$$

By substituting B in Eq. (2), the equation of velocity profile in the wake region is achieved as follow

$$U_w(y) = U_\infty - \frac{U_\infty C_d D}{2\delta\sqrt{\pi}} \exp(-(\frac{y}{\delta})^2) \qquad (20)$$

δ is dependent on the position of velocity measurement and consequently the velocity profile depends on x_m coordinate which is defined as the distance between body and measurement position. As can be seen from Eq. (20), U_w is a nonlinear function of the most important flow parameters. This equation is for mean flow conditions and all parameters are the time average.

3. SOLUTION OF THE INVERSE PROBLEM

In the inverse problem considered in this work, we are looking for the unknown parameters $[C_d, \delta, U_\infty]$. Direct measurement of these parameters is very costly and difficult. These parameters can be evaluated from velocity measurements taken at several downstream points in the wake region of flow field. It should be noted that free flow velocity can be measured too.

Upon the parameterization given by Eq. (20), the inverse problem has been formulated as a parameter estimation problem. The solution of the inverse problem for the estimation of the two unknown parameters is based on the minimization of the ordinary least squares norm of error function, which is defined by

$$e_j(\vec{P}, y_j) = d_j - U_w(\vec{P}, y_j) \qquad (21)$$

$$\text{Minimize}\left(S = \frac{1}{2}\sum_{j=1}^{N}\left[d_j - U_w(\vec{P}, y_j)\right]^2\right) \qquad (22)$$

Where e_j is the error function, d_j is the measured water velocity in the wake region and $U_w(\vec{P}, y_j)$ is the calculated velocity, which is the nonlinear function of unknown parameters $\vec{P}$. y_j is the vertical position of jth measurement point in the wake region. The vector of unknown parameters is formed by

$$\vec{P}^T = \{C_d, \delta\} \qquad (23)$$

We use the Levenberg–Marquardt method for parameter estimation, written in matrix form

$$\left(J^T J + \lambda I\right)\Delta \vec{P} = -J^T \vec{E} \qquad (24)$$

Where $\vec{E}$ is the vector of error function, I represents the identity matrix, J is the Jacobean matrix, λ is a damping coefficient to improve the convergence behavior and remove the ill-condition of Hessian matrix which is defined as below

$$H = J^T J \qquad (25)$$

The elements of the Jacobian matrix are

$$J_{mn} = \frac{\partial u_m}{\partial p_n}, \quad \begin{array}{l} m = 1, 2, \cdots, M \\ n = 1, 2, \cdots, N \end{array} \qquad (26)$$

Where u_m is the wake's velocity at vertical location of y_m and it can be defined as $u_m = U_w(y_m)$ and p_n is the nth unknown parameter. Equation (24) is then written in a form convenient to be used in an iterative procedure,

$$\Delta P^k = -\left(J^{kT}J^k + \lambda^k I^k\right)^{-1} J^{kT} \vec{E}^k \qquad (27)$$

Where k is the iteration index.

A new estimation of the parameters, $\vec{P}^{k+1}$, is calculated by

$$\vec{P}^{k+1} = \vec{P}^k + \Delta \vec{P}^k \qquad (28)$$

The iterative procedure starts with an initial guess for parameters, $\vec{P}^0$, and new estimates, $\vec{P}^{k+1}$, are sequentially obtained using Eq. (28) with $\Delta \vec{P}^k$ given by Eq. (24) until the convergence criterion is satisfied. It can be written as

$$\left|\frac{\Delta p_n^k}{p_n^k}\right| < \varepsilon, \quad n = 1, 2 \qquad (29)$$

Where ε is a small real number, such as 10^{-8}. The elements of the Jacobian matrix as well as the right hand term of Eq. (27) are calculated by using the Eq. (20), as described in the previous section. The damping coefficient λ must be changeable to modify the convergence optimally. In order to reach this aim, λ is set to a large value if Hessian matrix is non-positive definite, or to a small value if it is positive definite.

4. EXPERIMENTAL APPARATUS AND INSTRUMENTATION

The experiments are conducted in a water tunnel located in the Hydrodynamic Laboratory at the Iran University of Science and Technology (IUST). The water tunnel is of the closed-circuit type, and it has four aggregated, 1-m-long test sections (a total length of 4m) with a rectangular cross section of 0.1m × 0.2 m. The water's speed can be varied continuously. The turbulence intensity (TI) level in the free flowing stream is about 4.4%. A scaled pitot tube with electrically-controlled movement is used to measure the water's velocity.
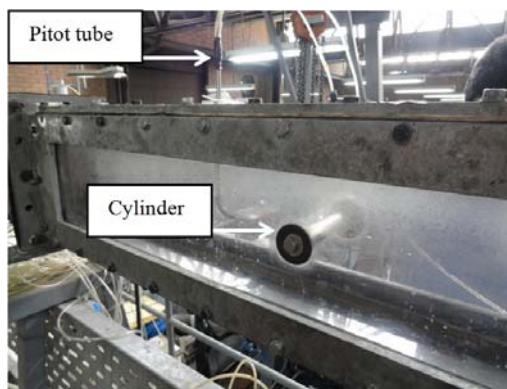

Fig. 2. Experimental Setup for measuring flow velocity of wake region.

Figure 2 shows the cylinder installed in one of the sections of the tunnel and the pitot tube which is used to measure the wake velocity. The pressure differences of the pitot tube are transmitted to a pressure measurement system (PMS) with 64 pressure-sensor channels. The output signals of the PMS are transmitted to a PC through a 12-bit data-acquisition card and are processed by Hydrolab Data Processing Software (HDPS). The outputs of HDPS consist of discrete dynamic and static pressures. Then, the water's velocity is calculated by using these pressure differences and the Bernoulli equation given below:

$$P + 0.5\rho v^2 + \rho g h = cet \qquad (30)$$

Where P is static pressure, ρ is the water's density, g is the gravity acceleration, v is water's velocity and h is the velocity head. A flow meter made by the Endress-Hauser Company (model: Proline Promag 10P) is used to measure the mean flow velocity.

An uncertainty analysis of the data is performed according to the procedure described by (Kline 1985). The uncertainty associated with the velocity measurements by the pitot tube is: $U_{uc} = 0.052$ m/s precision. To verify the results of the developed inverse method and because of the availability of hydrodynamic information for cylinders in several references, a cylinder with a 2-cm diameter and a 10-cm length is used as the investigated body in the flow field (Fig. 2). Four longitudinal velocity profiles are measured at stations located 10, 40, 60, and 80 cm from the centerline of the cylinder. These measurements are performed at 29 points for every section of the tunnel. Fig. 3 presents the grid distribution of velocity measurements. The distance between measurement points are 0.005m in the range of [-0.05, 0.05] and 0.01m in the ranges of [0.05, 0.095] and [-0.095, -0.05].
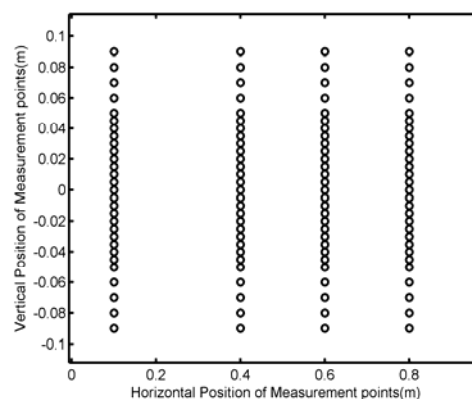

Fig. 3. Grid distribution of velocity measurements.

All of the profiles are measured over the centerline of the test section. For every section, the velocity profiles are measured three times, and the time average of them is used. The drag coefficient (C_d), wake's width (δ), and free flow velocity (U_∞), for each measured wake velocity profile are obtained

through a program specially developed in the MATLAB software package.

5. RESULT

The objective of this work is to estimate the unknown parameters introduced earlier. The closer the measurement location to the centerline of the water tunnel, the higher the resolution required for the measured velocities. This is due to the higher velocity gradient near the center of the body. This issue is performed in the grid distribution of velocity measurements. As stated before, the developed inverse algorithm is applicable for a moving body in the sea or in an environment without boundaries. Therefore, to reduce the effect of the tunnel's wall, several experiments are performed to determine the minimum distance from the wall at which the wall effect vanishes. Fig. 4 shows the free flow velocity that is measured by pitot tube in the water tunnel. As can be seen from this figure, in the range of [-0.05, 0.05] (m) from centerline of the cylinder, the wall or boundary layer effects almost vanish. Therefore, the data of the water velocities in the range of [-0.045, 0.045] are used in the estimation of the parameters. However, the effects of static pressure drop in the tunnel and turbulence intensity effects must be considered in the results of the study. As mentioned before water velocity is measured at 29 points in one section of the tunnel. Due to the wall effects, just 19 points of them are applicable for parameters estimations and the vertical distance between these points are 0.005m.
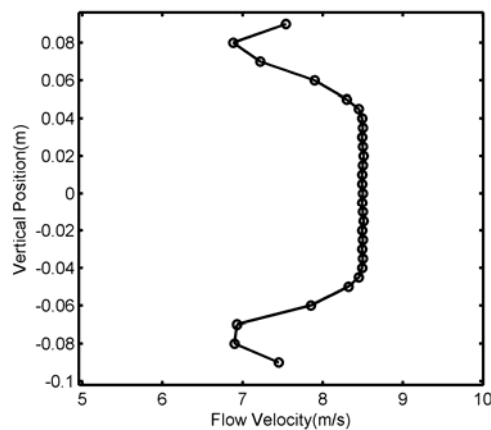

Fig. 4. Free flow velocity measured by pitot tube in the water tunnel.

Figure 5 shows the measured and fitted velocity profiles of the wake region at 10, 40, 60 and 80 cm from the centerline of the cylinder. It shows that a good conformity is achieved between the measured and fitted velocity profiles for all of the cases but the two last cases have the best coincidence. This is because of lower velocity gradient for two last cases. The closer to the body in the wake the higher resolution is needed to have a better-fitted profile. In these experiments, the free flow velocity is measured by a flow meter.
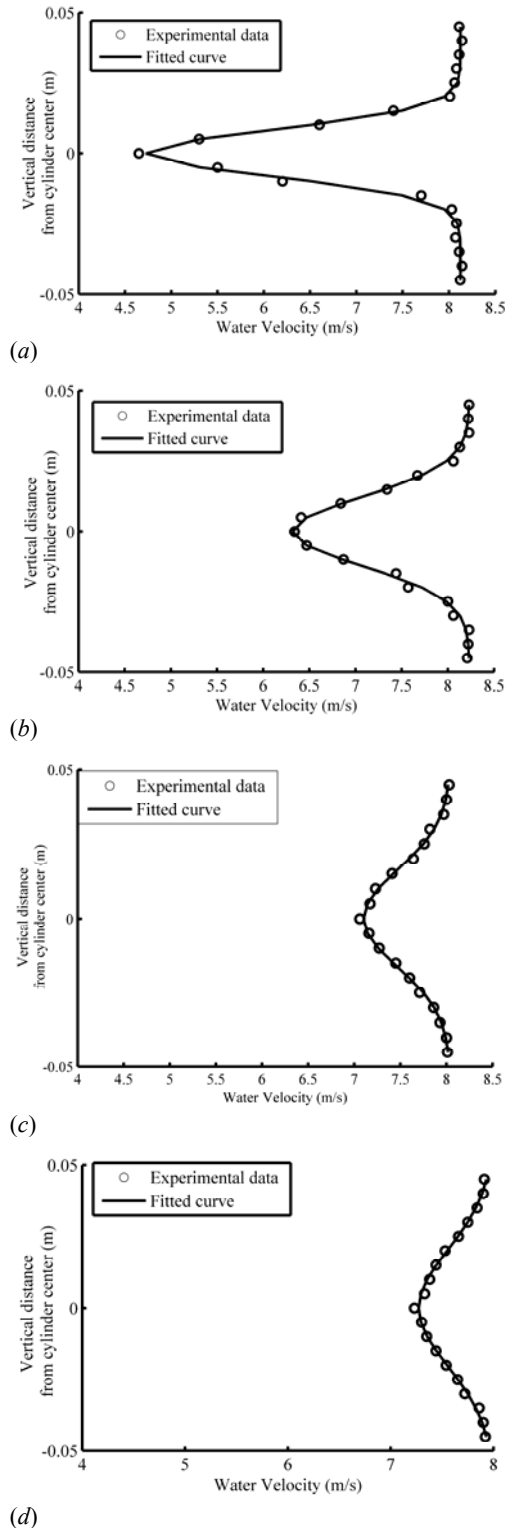

(a)

(b)

(c)

(d)

Fig. 5. Measured and fitted wake velocity profiles at (a) 10, (b) 40,(c) 60, (d) 80 cm from the center of the cylinder.

To develop the equation for the wake's velocity, it is assumed that the entrance and exit static pressures of the control volume are equal. However, this assumption is only true for an environment without boundaries. In the water tunnel, the static pressure decreases due to the friction and tangential

stress, and this must be taken into account in the estimation procedure. Thus, the upstream and downstream static pressures are measured for all the mentioned cases and the equivalent drag coefficients due to the pressure differences are evaluated and subtracted from the estimated drag coefficients by the inverse method.

Based on the findings of Schlichting, and Gersten, (2003), the drag coefficient for the cylinders with Reynolds numbers in the range of 1.6×10^5 to 1.7×10^5 in a boundary-less environment is almost 1.25. However, it is different for a water tunnel with a Turbulence Intensity (TI) of 4.4% (Li *et al.* 2009). Cheung and Melbourne (1980) demonstrated the dependency of the drag coefficient of a cylinder on TI and Reynolds number. Their results indicate that, for a TI of 4.4% and $R_e = 1.65 \times 10^5$ the drag coefficient is equal to 0.53.

Table 1 compares the estimated drag coefficient, $(C_d)_E$, for different wake velocity measurements with the drag coefficient values presented by Cheung and Melbourne. (1980), $(C_d)_R$, for the same Reynolds Numbers. Table 1 shows also the error of estimated drag coefficients, e_{Cd}.

Table 1 Comparison between estimated value for drag coefficient and its value presented by Cheung and Melbourne. (1980)

x_m, (cm)	$(C_d)_E$	$(C_d)_R$	e_{Cd}	R_e
10	0.67	0.53	37%	164000
40	0.59	0.53	11.3%	158400
60	0.52	0.53	1.88%	156800
80	0.535	0.53	1.9%	154600

As can be seen from Table 1 estimated drag coefficients for two last positions (i.e. x_m=60 and x_m=80) are evaluated accurately and have errors lower than 2%. This shows that the developed inverse method can estimate drag coefficient with an acceptable accuracy.

Table 2 shows the estimated wake's width δ_E, the measured, $(U_\infty)_M$, and estimated, $(U_\infty)_E$, velocity of free flow and their errors for different measurements.

Table 2 Estimated wake's width, measured and estimated velocity of free flow and their errors

x_m, (cm)	δ_E (m)	$(U_\infty)_M$ (m/s)	$(U_\infty)_E$ (m/s)	e_{U_∞}
10	0.021	8.20	8.21	0.12%
40	0.032	7.92	7.94	0.25%
60	0.037	7.84	7.81	0.38%
80	0.041	7.73	7.76	0.39%

As can be seen from Fig. 2, Table 1 and Table 2 the unknown parameters are estimated by the proposed inverse method accurately. As expected, the error of estimated drag coefficient, (e_{Cd}), showed that, in order to achieve accurate results, the measurement

position, (x_m), must be suitable. Choosing a proper location for velocity measurement depends on Reynolds number. The experimental results indicate that the distance range of $30D \leq x_m \leq 40D$ for the measurement location is suitable for the Reynolds number of 1.6×10^5 and the unknown parameters, especially C_d, can be estimated with good accuracy in this range of position. The estimated wake's widths can be compared with those extracted from the measured velocity profiles. Through this comparison, one can deduce that the estimated wake's widths have an acceptable accuracy. Finally, it is shown that the estimated values for drag coefficient (C_d), wake's width (δ), and free flow velocity (U_∞) by the developed inverse method have an acceptable accuracy and the presented model for wake velocity of flow can be used for estimation of drag coefficient.

All of the above results ensure that the present procedure can be extended to the estimation of drag force acting on the other kinds of bodies such as hydrofoils.

4. CONCLUSION

An inverse problem is formulated as a parameter estimation problem that searches drag coefficient, wake's width, and free flow velocity by measuring the wake velocity in an incompressible turbulent flow over an underwater body. The proposed method is applicable for two-dimensional flows. To examine the developed inverse method, several experiments are conducted to measure the wake velocity of the flow over a cylinder and the unknown parameters are identified. In the identification process, turbulent intensity, and pressure drop effects are undertaken.

By comparing our results with those of other researchers, it is shown that drag coefficient, wake's width, and free flow velocity values can be estimated accurately if appropriate experimental data are obtained by measuring the velocity profiles at suitable locations from the body.

All of the above results are very promising, which leads us to believe that the present approach can be extended for estimation of the drag force on the other kinds of underwater vehicles. Due to the great cost of direct measurement of the forces acting on these bodies, inverse methods could become powerful tools for evaluating these forces. This issue will be addressed in future work by the authors of this paper.

REFERENCES

Yang, S. Q. and D. H. Ding (2014). Drag-reducing flows in laminar-turbulent transition region. *J. Fluids Eng.* 136(10).

Akindoyo, E. O. and H. A. Abdulbari (2016). Investigating the drag reduction performance of rigid polymer–carbon nanotubes complexes. *Journal of Applied Fluid Mechanics* 9(3), 1041-1049.

Alifanov, O. M. (1994). *Inverse Heat Transfer Problems*. Springer Berlin Heidelberg, New York.

Amromin, E. L., (2013), Vehicles Drag Reduction with Control of Critical Reynolds Number. *J. Fluids Eng*, 135(10).

Cheung, C. K. and W. H. Melbourne (1980, August). Wind Tunnel Blockage Effects on a Circular Cylinder in Turbulent Flows. In *Proceeding of 7th Australasian Hydraulics and Fluid Mechanics Conference*, Brisbane.

Cho .H., F. E. Udwadia (2012). Inverse Problem for Lagrangian Dynamics for Multi-Degree-of-Freedom Systems with Linear Damping, 601-608.

Ghassabi, G. and M. Kahrom (2015). Investigating Flat Plate Drag Reduction using Taguchi Robust Design. *Journal of Applied Fluid Mechanics* 8(4), 855-862.

Grysa, K., A. Maciag and J. A. Krasa (2014). Trefftz functions applied to direct and inverse non-Fourier heat conduction problems. *J. Heat Transfer* 136(9).

Jafargholinejad, S., A. Pishevar and K. Sadeghy (2011). On the use of rotating-disk geometry for evaluating the drag-reducing efficiency of polymeric and surfactant additives. *Journal of Applied Fluid Mechanics* 4(2), 1-5.

Jordan, S. A. (2014). Understanding tow tank measurements of total drag for long thin circular cylinders. *J. Fluids Eng* 136(3).

Kline, S. J. (1985). The Purpose of Uncertainty Analysis. *ASME J. Fluids Eng* 107 (2), 153-160.

Li, C. G., C. K. Cheung- John and Z. Q. Chen (2009, November). Effect of square cells in improving wind tunnel flow quality. In *Proceedings of the 7th Asia-Pacific Conference on Wind Engineering*, Tamkang University, Taipei, Taiwan.

Morton. C. and S. Yarusevych (2014). Vortex dynamics in the turbulent wake of a single step cylinder. *J. Fluids Eng*. 136.

Nili-Ahmadabadi, M., A. Hajilouy-Benisi, F. Ghadak and M. Durali (2010). A novel 2D incompressible viscous inverse design method for internal flows using flexible string algorithm. *J. Fluids Eng* 132(3).

Orlande, H. R. (2012). Inverse problems in heat transfer: new trends on solution Methodologies and applications. *J. Heat Transfer* 134(3).

Ozisik, M. N. and H. R. B. Orlande (2000). *Inverse Heat Transfer: Fundamentals and Applications.* Taylor and Francis, New York.

Sakly, A., A. Jemni1, P. Lagonotte and D. Petit (2011). Estimation of the effective thermal properties in a metallic medium by an inverse technique using temperature measurements. *Journal of Applied Fluid Mechanics* 4(4), 23-29.

Schlichting, H. and K. Gersten (2003). *Boundary-Layer Theory*. Institute for Thermodynamics and Fluid Mechanics. D-44801, Bochum, Germany.

Su, J. and A. J. Silva Neto (2001). Simultaneous estimation of inlet temperature and wall heat flux in turbulent circular pipe flow. *Numerical Heat Transfer*, *Part A* 40 (7), 751-766.

Su, J., A. B. Lopes and A. J. Silva Neto (2000). Estimation of unknown wall heat flux in turbulent circular pipe flow. *Int. Communication in Heat and Mass Transfer* 27 (7), 945-954.

Wosnik, M. and R. E. A. Arndt (2013). Measurements in high void-fraction bubbly wakes created by ventilated supercavitation. *J. Fluids Eng*. 135(1).

Wu, X., M. Wendel, G. Chahine and B. Riemer (2014). Gas bubble size measurements in liquid mercury using an acoustic spectrometer. *J. Fluids Eng*. 136(3).

Yang, W. and R. Xiao (2013). Multi-objective optimization design of a pump–turbine impeller based on an inverse design using a combination optimization strategy. *J. Fluids Eng*. 136(1).